

## Article

# *Streptomyces* spp. Isolated from *Rosa davurica* Rhizome for Potential Cosmetic Application

Shengdao Zheng<sup>1</sup>, Sarang Oh<sup>1</sup>, Minzhe Fang<sup>2</sup>, Arce Defeo Bellere<sup>2</sup> , Jeyong Jung<sup>2</sup>, Trang Thi Minh Nguyen<sup>2</sup> ,  
Jeehaeng Jeong<sup>1</sup> and Tae-Hoo Yi<sup>2,\*</sup> 

<sup>1</sup> Snowwhitefactory Co, Ltd., 807 Nonhyeon-ro, Gangnam-gu, Seoul 06032, Republic of Korea

<sup>2</sup> Graduate School of Biotechnology, Kyung Hee University, 1732 Deogyong-daero, Giheung-gu, Yongin-si 17104, Republic of Korea

\* Correspondence: drhoo@khu.ac.kr; Tel.: +82-31-201-3693

**Abstract:** *Streptomyces* species are widely studied and used in different fields, including antibiotics and pesticides, and are spread in several places as soil-derived microorganisms. However, research on anti-aging, including antioxidants obtained from *Streptomyces*, has not been performed as much. Skin aging due to bacterial infection, especially methicillin-resistant *Staphylococcus aureus* (MRSA), is challenging to recover, so it is essential to prevent aging by preventing or inhibiting infection. Therefore, this study was conducted to isolate *Streptomyces* species from *Rosa davurica* rhizome soil and to determine the effect of the ethyl acetate extract of the isolated strain *Streptomyces chattanoogensis* THA-663 (THA-663S) on the inhibition of MRSA and UVB-irradiated human skin keratinocytes, to determine whether it could be a treatment for skin aging. The MRSA inhibition and antioxidant activities were evaluated using disc diffusion, 2,2-diphenyl-1-picrylhydrazyl (DPPH), 2,2'-azino-bis-(3-ethylbenzothiazoline)-6-sulfonic acid (ABTS), and a reactive oxygen species (ROS) assay. The expression of aging-related markers, including mitogen-activated protein kinases/activator protein 1 (MAPK)/AP-1 and transforming growth factor- $\beta$ /suppressor of mothers against decapentaplegic (TGF- $\beta$ /Smad) was assessed using Western blotting. The antibacterial effect on four MRSA strains, CCARM 0204, CCARM 0205, CCARM 3855, and CCARM 3089, showed that THA-663S could greatly inhibit MRSA growth. Moreover, the findings showed that THA-663S is efficient in scavenging free radicals and dose-dependently reducing ROS generation. Furthermore, THA-663S notably reduced UVB-induced matrix metalloproteinase-1 (MMP-1) expression by inhibiting the MAPK/AP-1 signaling pathways and blocking extracellular matrix (ECM) degradation in UVB-irradiated HaCaT cells. Additionally, THA-663S improved and enhanced transforming growth factor-beta (TGF- $\beta$ ) signaling activation to promote procollagen type I synthesis, relieving UVB-induced skin cell damage. In conclusion, THA-663S has a high potential to protect skin cells from aging, and, simultaneously, it can prevent or treat aging caused by infection due to pathogen inhibition.

**Keywords:** *Streptomyces chattanoogensis* THA-663 extract (THA-663S); anti-aging; antibacterial; methicillin-resistant *Staphylococcus aureus* (MRSA)



**Citation:** Zheng, S.; Oh, S.; Fang, M.; Bellere, A.D.; Jung, J.; Nguyen, T.T.M.; Jeong, J.; Yi, T.-H. *Streptomyces* spp. Isolated from *Rosa davurica* Rhizome for Potential Cosmetic Application. *Cosmetics* **2022**, *9*, 126. <https://doi.org/10.3390/cosmetics9060126>

Academic Editor: Enzo Berardesca

Received: 31 October 2022

Accepted: 21 November 2022

Published: 25 November 2022

**Publisher's Note:** MDPI stays neutral with regard to jurisdictional claims in published maps and institutional affiliations.



**Copyright:** © 2022 by the authors. Licensee MDPI, Basel, Switzerland. This article is an open access article distributed under the terms and conditions of the Creative Commons Attribution (CC BY) license (<https://creativecommons.org/licenses/by/4.0/>).

## 1. Introduction

Skin aging is divided into endogenous and exogenous, and, unlike inevitable endogenous aging, there are different factors in exogenous aging [1]. Among them, skin infections caused by microorganisms and skin aging caused by UVB exposure account for the largest proportion [2]. UVB exposure evokes complex and multifaceted signal networks that promote intracellular ROS formation, which in turn damages the lipids, proteins, and nucleic acids in keratinocytes [2]. Additionally, UV exposure increases epidermal thickness, decreases collagen synthesis, and facilitates collagenolysis by upregulating the expression of matrix metalloproteases (MMPs) [3]. UVB-induced ROS activates mitogen-activated

protein kinase (MAPK) signaling, which further induces MMPs and eventually promotes collagen degradation [4,5].

In the skin, the impairment of type I procollagen by inducing collagen fibrils depends on the expression of MMP-1 (matrix metalloproteinase1), a zinc-dependent endopeptidase that degrades type I collagen specifically [5]. It is regulated mainly by the upper signaling cascades, including MAPKs, extracellular signal-regulated kinase (ERK), c-Jun N-terminal kinase (JNK), and p38 [6]. After activation of the MAPKs by UV, transcription factor (AP-1) expression increases, causing fragmentation, inflammatory response, and cell death [7,8]. Additionally, NF- $\kappa$ B, another critical transcription factor of MMP in the dermis, is translocated under photodamaged conditions into the nucleus by degradation of I $\kappa$ B and elevates MMP and pro-inflammatory cytokines, including TNF- $\alpha$ , IL-1 $\beta$ , and IL-6 [9,10]. Interestingly, UVB not only changes the collagen-degradation pathway but also the synthesis pathway, transforming growth factor- $\beta$ /suppressor of mothers against decapentaplegic (TGF- $\beta$ /Smad). The TGF- $\beta$ /Smad pathway involves a reduction in T $\beta$ RII level and the phosphorylation of Smad3; the downstream signaling is significantly reduced in photoaged human skin [11,12]. Impairment of the TGF- $\beta$ /Smad pathway is also a mechanism causing collagen loss. Due to complicated changes in different pathways, the ECM collapses, causing wrinkle formation.

*Streptomyces* is a genus of Gram-positive bacteria that grows in different environments, with a filamentous form similar to fungi. The most interesting quality of *Streptomyces* is its ability to produce bioactive secondary metabolites, including antifungals, antivirals, antitumoral, antihypertensives, and mainly antibiotics and immunosuppressives [13]. Moreover, recent reports suggest that *Streptomyces* species produce metabolites with strong antioxidant activity that can be developed as different therapeutic agents; most *Streptomyces* species have antibacterial effects [14]. MRSA is a major causative pathogen that causes skin infection, and, even if infected, the amount and time of use are limited by considering antibiotic resistance and sensitization. MRSA exhibits resistance to more diverse antibiotics over generations and is becoming harder to treat [15]. The skin infection caused by an MRSA infection seems to be more vital in prevention and suppression than treatment.

*Rosa davurica* has long been used as a traditional Chinese herbal therapy for diseases because of its high antioxidant, antiviral, and anti-inflammation characteristics. In addition, according to a recent study, it has been reported to have a very excellent effect on anti-aging [16]. Therefore, this study conducted experiments using *Streptomyces chattanoogensis* separated from *R. davurica* rhizome soil, focusing on the prevention and recovery of skin aging caused by UV and bacterial infection to check the value as a treatment.

## 2. Materials and Methods

### 2.1. Chemicals and Reagents

Human keratinocytes (HaCaT cells) were purchased from the Republic of Korea cell line bank (Seoul, Republic of Korea). Dulbecco's Modified Eagle's Medium (DMEM), fetal bovine serum (FBS), antibiotics, and the antimycotic were supplied by Hyclone Laboratories Inc. (Marlborough, MA, USA) and Gibco RBL (Grand Island, NY, USA), respectively. Ascorbic acid, 3-(4,5-dimethylthiazol-2-yl)-2,5-diphenyltetrazolium bromide (MTT), dimethyl sulfoxide (DMSO), ampicillin, gentamycin, norfloxacin, natamycin, and Mueller Hinton Agar (MHA) media were purchased from Sigma-Aldrich (St. Louis, MO, USA). ELISA kits for detecting human MMP-1 and MMP-3 were purchased from R&D Systems (Minneapolis, MN, USA). The primary and secondary antibodies were obtained from Cell Signaling Technology (Beverly, MA, USA), Santa Cruz Biotechnology (Santa Cruz, CA, USA), and Bio-Rad Laboratories, Inc. (Hercules, CA, USA). International *Streptomyces* project (ISP) media 2 and Starch Casein Agar (SCA) were purchased from KisanBio (Seoul, Republic of Korea). All other materials were obtained from normal commercial sources and were of the highest grades available.

## 2.2. Identification of Strain THA-663

One gram of soil samples was dissolved in 9 mL of distilled water and diluted serially by 10-fold dilution up to  $10^{-6}$  dilution and spread onto SCA. The plates were incubated at 30 °C for 7 days then the single colony was picked up to repeat again for purification. Identification of strain THA-663 is by 16S rRNA sequencing results provided by Biofact co., Ltd (Daejeon, Republic of Korea). Based on the sequencing result, the phylogenetic tree was drawn by MEGA X program, and the highest similarity of two strains, *Streptomyces chattanoogensis* NRRL ISP-5002 (KACC 14678) and *Streptomyces lydicus* ATCC 25470 (KACC 21074), were received from Korean Agricultural Culture Collection (KACC) for the taxonomy experiments. Three strains were inoculated at the same time with the same conditions and checked for growth in different pH, temperature, NaCl concentration and for susceptibility to different antibiotics with antibiotics strips.

## 2.3. Liquid–Liquid Extraction (LLE)

This study was conducted by modifying the methods of Flårdh, K. et al. [17] and Davoodbasha, M. et al. [18]. *S. chattanoogensis* THA-663 was isolated from *Rosa davurica* rhizome soil; the strain was inoculated into 50-mL ISP 2 medium and incubated in a shaking incubator with 160 rpm, 30 °C conditions for seven days as a seed culture. Then, it was inoculated into 5-L ISP 2 medium (1%, v/v) for another seven days in the same conditions and centrifuged at  $19,000 \times g$  at 4 °C for 20 min. Then, it was filtered with a 0.22- $\mu$ m bottle-top vacuum filter. An equal volume of ethyl acetate was added and repeated thrice (more than three hours each time) and evaporated using a vacuum rotary evaporator in 40 °C, and crude extract THA-663S was collected.

## 2.4. Identification of Components by UPLC-Qtof-MS

UPLC-Qtof-MS was performed with a reversed-phase UPLC gradient (Waters Acquity<sup>®</sup> FTN, Acquity BSM) coupled with a waters Vion<sup>™</sup> IMS-Qtof mass spectrometer, operated in positive-ion electrospray mode with mobility-enabled non-targeted HDMSE scan methods, with the range of 50–2000 Da using 0.1 sec scan time. The chromatographic separation was achieved with gradient elution at a flow rate of 0.35 mL/min using 0.1% formic acid in methanol/water (10: 90, v/v) as mobile phase A and 0.1% formic acid in methanol/water (90: 10, v/v) as mobile phase B. The elution conditions were as follows: 0–1 min, 5% B; 1–14 min, 5–50% B; 14–18 min, 50–98% B; 18–22 min, 98% B; 22.5–25 min, 98–5% B. The detection wavelength was 254 and 320 nm. MS low and high collision energies were 6 and 20–40 eV, respectively. Nitrogen was used as the drying gas. Desolvation gas flow was 800 L/h, and the cone gas flow was maintained at 50 L/h. Desolvation temperature was 400 °C, and source temperature was 150 °C. Observed capillary and sampling cones were 3.5 KV and 30 V, respectively. Reference capillary was set at 2.0 KV. Data acquisition and processing were conducted by UNIFI v1.8.1.

## 2.5. DPPH and ABTS Radical Scavenging Activity

The antioxidant actions of THA-663S were examined. The 2,2-diphenyl-1-picrylhydrazyl (DPPH, PubChem CID: 2375032) and 2,2'-azino-bis-(3-ethylbenzothiazoline)-6-sulfonic acid (ABTS, PubChem CID: 5464076) assays were used for scavenging activity against free radicals. The absorbance of 0.1 mM DPPH solution in 80% (v/v) methanol was set at  $0.650 \pm 0.02$  at 517 nm. The reaction of the mixture of solution and diluted sample with various concentrations (satisfied the standard curve) was processed at 37 °C for 30 min for DPPH and 10 min for ABTS. The absorbance descent resulted from radical scavenging capacity and was read using a microplate reader at 595 nm and 405 nm. The radical scavenging activity of the sample was evaluated using the following formula:

$$\text{DPPH and ABTS radical inhibition (\%)} = \frac{(\text{OD}_0 - \text{OD}_x)}{\text{OD}_0} \times 100$$

with  $OD_0$  being the optical density measured for the negative control and  $OD_x$  measuring for the different THA-663S or ascorbic acid concentrations.

Inhibitory concentration ( $IC_{50}$ ) was calculated by applying GraphPad Prism (version 7.0, La Jolla, CA, USA).

### 2.6. Antibacterial Activity

The cell-free supernatant extract was dissolved in MeOH. The standard disc diffusion method was conducted [19]. Sterilized Petri dishes were prepared using Mueller Hinton Agar (Oxoid, UK) [20]. Pathogen indicator bacteria MRSA strains ( $1 \times 10^6$  CFU/mL) were inoculated into MHA plates. Exactly 100  $\mu$ L of dissolved extract was loaded onto Whatman No. 1 sterile filter paper disk (8 mm diameter) and allowed to dry for 30 min. The negative control was MeOH. Dried paper disks are placed on the plate. Afterward, the plates were cultured at 30 °C for 24 h. Antimicrobial activity was assessed by measuring the zone of inhibition against the tested bacteria [21].

Methicillin-resistant *Staphylococcus aureus* (MRSA) was received from Seoul Women's University for anti-MRSA activity (Supplementary Table S1). The inhibition zone was measured using the same technique for screening pathogenic bacteria to check the effect of *S. chattanoogensis* THA-663 on MRSA. Positive controls are Ampicillin (Amp), Gentamycin (GM), Norfloxacin (Nor), and Natamycin (Nat).

### 2.7. MIC and MBC

The minimum inhibitory concentration (MIC) and minimum bactericidal concentration (MBC) of the crude extract of *S. chattanoogensis* THA-663 used the dilution method described by Kirby–Bauer. One milliliter of each Nutrient Broth (0.5% peptone, 0.3% beef extract, 0.5% yeast extract, and 0.5% NaCl) was added to the prepared tube, and 20 mL crude extract was prepared by dissolving in methanol and was added only to the first tube, followed by two-fold dilution. Then, 100- $\mu$ L indicators, including *S. aureus*, were added to each tube, so that the final concentration is  $1 \times 10^6$  CFU/mL, and were incubated at 37 °C for 24 h. The MBC was determined to be the concentration in test samples, where it exhibited no visual growth of the indicators. The MIC was determined to be the concentration in test samples, which decreased the visual growth of the indicators.

### 2.8. Cell Culture and Treatment

HaCaT cells were grown in an incubator at 37°C under a humidified atmosphere containing 5% CO<sub>2</sub>. DMEM supplemented with 10% heat-inactivated FBS and 1% antibiotics and antimycotic solution was used for cell culture. To mimic the photoaging process, after HaCaT cells reached 80% cell confluence, cell plates with closed lids were exposed to UVB (125 mJ/cm<sup>2</sup>) radiation using UVB irradiation machine (Bio-Link BLX-312; Vilber Lourmat GmbH, France). Then, fresh serum-free medium containing 10  $\mu$ M ascorbic acid (positive control) or three doses of THA-663S (0.1, 1, and 10  $\mu$ g/mL) was added to each plate for incubation.

### 2.9. Cell Viability

Cell viability was measured by 3-(4,5-dimethylthiazol-2-yl)-2,5-diphenyltetrazolium bromide (MTT, Sigma-Aldrich, St. Louis, MO, USA) assay. The effects of THA-663S on the viability of HaCaT cells were evaluated by MTT assay. After UVB (125 mJ/cm<sup>2</sup>) radiation, HaCaT cells were treated with THA-663S (0.1, 1, and 10  $\mu$ g/mL) in serum-free medium. After 24 h, the medium was removed and replaced with 30  $\mu$ L of MTT (1 mg/mL) for 4 h, and DMSO was added to dissolve the formazan crystals.

### 2.10. Reactive Oxygen Species (ROS) Scavenging Activity

HaCaT cells were exposed to UVB irradiation (125 mJ/cm<sup>2</sup>) and then treated with the indicated concentrations of THA-663S (0.1, 1, and 10  $\mu$ g/mL) and ascorbic acid (10  $\mu$ M) for 24 h. The cells were then rinsed twice with PBS and stained with 30  $\mu$ M 2',7'-dichloro-

fluorescein diacetate (DCFH-DA; Sigma-Aldrich) for 30 min at 37 °C in a CO<sub>2</sub> incubator. The ROS production was analyzed by flow cytometry (BD Accuri C6; Becton-Dickinson, San Jose, CA, USA).

#### 2.11. Enzyme-Linked Immunosorbent Assay (ELISA)

The secretion of cytokines was quantified with commercial ELISA kits. HaCaT cells were exposed to UVB irradiation (125 mJ/cm<sup>2</sup>) and then treated with the indicated concentrations of THA-663S (0.1, 1, and 10 µg/mL) and ascorbic acid (10 µM) for 24 h. The cell medium was collected from each well to detect the levels of MMP-1 and MMP-3 by using ELISA kits.

#### 2.12. Reverse Transcription Polymerase Chain Reaction (RT-PCR) Analysis

HaCaT cells were exposed to UVB irradiation (125 mJ/cm<sup>2</sup>) and then treated with the indicated concentrations of THA-663S (0.1, 1, and 10 µg/mL) and ascorbic acid (10 µM) for 24 h. The total RNA was isolated from HaCaT cells, in accordance with the instructions of the manufacturer, by TRIzol reagent (Invitrogen Life Technologies, Carlsbad, CA, USA). The RNA (3 µg) was reverse-transcribed with 200 units of reverse transcriptase and 0.5 µg/µL oligo-(dT)15 primer (Bioneer Co., Daejeon, Republic of Korea). This reaction was performed at 70 °C for 5 min and at 42 °C for 60 min and was terminated at 94 °C for 5 min. The PCR amplification was performed with a PCR premix (Bioneer Co., Daejeon, Republic of Korea), and the primers used in this reaction were described in PCR amplification that was performed using a PCR premix (Bioneer) and designated as primer pairs in Supplementary Table S2. PCR products were separated by gel electrophoresis on 2% agarose gels and visualized with nucleic acid staining (Noble Bio Inc., Hwaseong-si, Republic of Korea) under UV illumination. GAPDH was used for normalization.

#### 2.13. Western Blot Analysis

To investigate the effects of THA-663S on MAPK/AP-1 and TGF-β/Smad signaling pathway expression in the HaCaT cells, it was exposed to UVB irradiation (125 mJ/cm<sup>2</sup>) and then treated with the indicated concentrations of THA-663S (0.1, 1, and 10 µg/mL) and ascorbic acid (10 µM). The total protein was lysed, and equivalent protein concentrations were performed with Pierce™ BCA Protein Assay Kit (Thermo Scientific, Waltham, MA, USA). Then, the proteins were subjected to SDS-PAGE (10–15% gel) under reducing conditions. Proteins were transferred to polyvinylidene fluoride (PVDF) membranes, and the membranes were blocked in PBS with 0.01% Tween 20 (PBST) containing 5% non-fat dried milk for 1 h at room temperature. Then, incubated primary antibodies and secondary antibodies were. After that, the film was developed by enhanced chemiluminescence (ECL). Film densitometry was performed using an imaging system (Fujifilm, LAS-4000, Tokyo, Japan).

#### 2.14. Statistical Analysis

The data were analyzed using Statistical Analysis System (GraphPad Prism 7.0). All the quantitative data are expressed as means ± SDs. The significance of differences was determined using a one-way analysis of variance (ANOVA) with the Student–Newman–Keuls test for multiple comparisons. Statistical significance was considered for  $p < 0.05$ . All experiments were performed independently three times.

### 3. Results

#### 3.1. Molecular Phylogenetic Identification

The 16S rRNA sequencing results provided by Biofact co., Ltd. showed the strain *S. chattanoogensis* THA-663 was closely related to *Streptomyces lydicus* ATCC 25470 (99.85% sequence similarity), *Streptomyces chattanoogensis* NRRL ISP-5002 (99.85%), and *Streptomyces sioyaensis* NRRL B-5408 (99.34%).

The results of the optimum growing conditions show that strain THA-663 is close to *S. chattanoogensis* (Table 1). The following results show the susceptibility of *S. chattanoogensis* THA-663 and two types of the most-related strains to antibiotics. Nine antibiotic strips, kanamycin, ampicillin, erythromycin, streptomycin, vancomycin, clindamycin, gentamycin, tetracycline, and chloramphenicol, were used for checking. The results of study showed a relatively large difference in MIC in erythromycin, clindamycin, and tetracycline (Table 2).

**Table 1.** Differences in pH, temperature and NaCl concentration.

Characteristic	THA-663	KACC 14678 <sup>2</sup>	KACC 21704 <sup>3</sup>
pH range	5–9	5–9	5–9
Optimum pH	6–7	6–7	6–8
10 °C	-	W <sup>1</sup>	-
30 °C	+	+	+
37 °C	+	+	+
Optimum temperature	30	30	37
Maximum NaCl con. (% w/v)	4%	6%	4%

<sup>1</sup> weak growth, <sup>2</sup> *S. chattanoogensis* KACC 14678, <sup>3</sup> *S. lydicus* KACC 21074.

**Table 2.** Minimum inhibitory concentration (MIC) for antibiotics.

Antibiotics	THA-663	KACC 14678 <sup>1</sup>	KACC 21074 <sup>2</sup>
Kanamycin	1.0	1.0	1.5
Ampicillin	>256	>256	_1)
Erythromycin	1.5	0.38	0.38
Streptomycin	0.5	0.5	0.75
Vancomycin	0.38	0.38	0.38
Clindamycin	48	1.5	0.25
Gentamycin	0.38	0.25	0.38
Tetracycline	48	8	32
Chloramphenicol	-	>256	-

Concentration: µg/mL, number mean: the concentration of antibiotics, -: no clear zone; <sup>1</sup> *S. chattanoogensis* KACC 14678, <sup>2</sup> *S. lydicus* KACC 21074.

A neighbor-joining tree indicated that the phylogenetic relationships between the representative actinobacteria and the type strains of the related genus *Streptomyces* are based on 16S rRNA gene sequences (Figure 1).

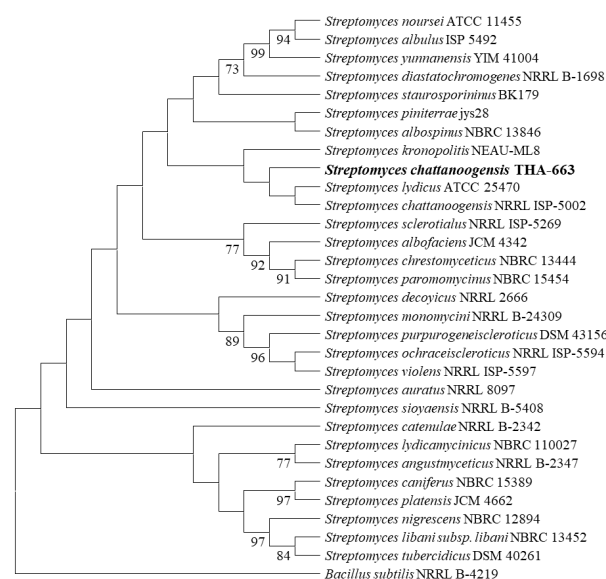


**Figure 1.** Phylogenetic tree of *S. chattanoogensis* THA-663. Bootstrap percentages (1000 replicates) above 70% are shown at the nodes and toggle-scaled the tree.

### 3.2. Antimicrobial Activity of THA-663S on Methicillin-Resistant *Staphylococcus aureus* (MRSA)

First, 5 L of liquid media with a 2.0 McFarland standard was extracted by ethyl acetate and finally 200 mg of crude extract THA-663S was obtained, which was tested for antibacterial activity compared to antibiotics such as ampicillin, norfloxacin, gentamicin, and natamycin by the modified disc diffusion technique. As a result, THA-663S indicated a large clear zone against MRSA bacteria such as *S. aureus* 285 CCARM 0204, *S. aureus* 503 CCARM 0205, *S. aureus* CCARM 3855, and *S. aureus* CCARM 3089 more than antibiotics. The results of antibacterial activity are expressed in Table 3. Norfloxacin cannot but ampicillin and gentamycin can less against MRSA. The concentration of THA-663S is 10 mg/mL, and the antibiotics concentrations are 2 µg/mL of ampicillin, 1 µg/mL of norfloxacin, 0.25 µg/mL of gentamicin, and 2 µg/mL of natamycin.

**Table 3.** Antibacterial effect of THA-663S on MRSA.

Microorganisms	Collection Code No.	THA-663S	AMP <sup>1</sup>	NOR <sup>2</sup>	GEN <sup>3</sup>	NAT <sup>4</sup>
<i>S. aureus</i> 285	CCARM 0204	1.31 ± 0.4%	-	-	1.1 ± 0.1%	-
<i>S. aureus</i> 503	CCARM 0205	1.36 ± 0.3%	-	-	1.02 ± 0.2%	-
<i>S. aureus</i>	CCARM 3855	1.02 ± 0.4%	1.39 ± 0.1%	-	-	-
<i>S. aureus</i>	CCARM 3089	1.01 ± 0.2%	-	-	-	-

Diameter unit: cm, -: negative, <sup>1</sup> Ampicillin, <sup>2</sup> Norfloxacin, <sup>3</sup> Gentamycin, <sup>4</sup> Natamycin.

### 3.3. Identification of Components in THA-663S by UPLC-Qtof-MS

The identification of THA-663S was performed on the basis of the analytical ion chromatogram from the measurement of tea samples using UPLC-Qtof-MS. To achieve the consistency of the retention times of different compounds in different analytical samples, the tea extract was analyzed under the same separation conditions as used for the in situ measurements. The identification of the compounds was compared with the mass spectra from the UNIFI traditional medicine library. As shown in Table 4, seven components were identified. The mass error for each compound was below 2 ppm of 3,6,9-Trimethyl-benzo[de]chromene (CHEMBL184245), 2-(4-Methoxybenzylidene)malonic acid (CHEMBL2148184), (5S)-5-Acetylaminoethyl-3-[4-acetyloxyacetylphenyl]oxazolidin-2-one (CHEMBL83512), 1H-Indole,3-(1E)-1-propen-1-yl- (CHEMBL1812532), kenganthranol A, [(2-Methoxyphenyl)carbamoyl]methyl 3-chloroadamantane-1-carboxylate (CHEMBL1484171), and 7-[(2S,3R,4S,5R,6R)-3,5-dihydroxy-6-(hydroxymethyl)-4-[(2S,3R,4R,5R,6S)-3,4,5-trihydroxy-6-methyloxan-2-yl]oxyoxan-2-yl]oxy-5-hydroxy-3,6-dimethoxy-2-(4-methoxyphenyl)chromen-4-one (CHEMBL2299266).

**Table 4.** List of components in THA-663S identified by UPLC-Qtof-MS.

No.	Component Name	Observed RT (min)	Formula	Observed <i>m/z</i>	Mass Error (mDa)	Adducts
1	3,6,9-Trimethyl-benzo[de]chromene	1.29	C <sub>15</sub> H <sub>14</sub> O	233.0940	0.3	+Na
2	2-(4-ethoxybenzylidene)malonic acid	2.25	C <sub>11</sub> H <sub>10</sub> O <sub>5</sub>	223.0598	-0.3	+H
3	N-[[3-[3-fluoro-4-(3-methyl-1,2,4-oxadiazol-5-yl)phenyl]-2-oxo-1,3-oxazolidin-5-yl]methyl]acetamide	3.58	C <sub>16</sub> H <sub>18</sub> N <sub>2</sub> O <sub>6</sub>	335.1226	-1.2	+H
4	1H-Indole, 3-(1E)-1-propen-1-yl-	3.80	C <sub>11</sub> H <sub>11</sub> N	158.0964	0.0	+H
5	Kenganthranol A	4.17	C <sub>25</sub> H <sub>28</sub> O <sub>5</sub>	431.1810	-1.9	+Na
6	[(2-Methoxyphenyl)carbamoyl]methyl 3-chloroadamantane-1-carboxylate	6.56	C <sub>20</sub> H <sub>24</sub> ClNO <sub>4</sub>	378.1452	-1.5	+H
7	7-[(2S,3R,4S,5R,6R)-3,5-dihydroxy-6-(hydroxymethyl)-4-[(2S,3R,4R,5R,6S)-3,4,5-trihydroxy-6-methyloxan-2-yl]oxyoxan-2-yl]oxy-5-hydroxy-3,6-dimethoxy-2-(4-methoxyphenyl)chromen-4-one	9.88	C <sub>30</sub> H <sub>36</sub> O <sub>16</sub>	653.2083	0.7	+H

### 3.4. DPPH and ABTS Radical Scavenging Activity

The antioxidant capacity of THA-663S was evaluated through DPPH and ABTS assay, and a positive control, such as ascorbic acid, was measured into IC<sub>50</sub> values. Ascorbic acid is a well-known antioxidant compound used as a reference standard and has strong DPPH and ABTS radical scavenging activities. As indicated in Figure 2, the IC<sub>50</sub> values of ascorbic acid needed for exerting its scavenging activity on DPPH and ABTS radicals were 653.1 and 356.4 ppm, respectively. THA-663S also significantly inhibited DPPH radicals, with an IC<sub>50</sub> value of 521.2 ppm, and ABTS radicals, with an IC<sub>50</sub> value of 160.5 ppm, proposing that THA-663S possesses potent antioxidant qualities.

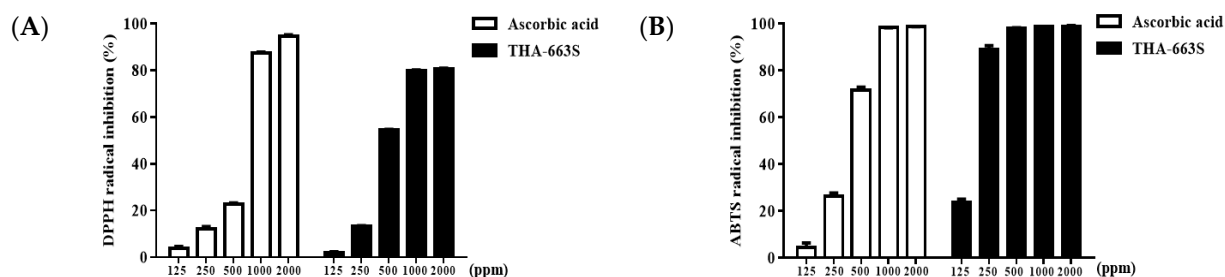


**Figure 2.** DPPH and ABTS radical scavenging activity of THA-663S. DPPH radical (A) and ABTS+ cation (B) scavenging activity of THA-663S. The radical scavenging effect was presented as a percentage measured in the control group. Ascorbic acid serves as a positive control. IC<sub>50</sub> values measured for ascorbic acid scavenging activity on DPPH and ABTS radicals were 521.2 and 160.5 ppm, respectively. The results are shown as the mean  $\pm$  SD of three independent experiments.

### 3.5. MIC and MBC

The antimicrobial activity of THA-663S was examined using a broth dilution assay. The cell growth of inhibitors was evaluated by visually verifying and measuring absorbance at 600 nm using a UV detector. As a result, THA-663S can inhibit MRSA growth at concentrations of 1.25–5 mg/mL (Table 5).

**Table 5.** MIC and MBC of THA-663S to multi-drug-resistant bacteria.

Gram	Microorganisms	Collection Code No.	MIC	MBC
Gram-positive	<i>S. aureus</i> 285	CCARM 0204	2.5	5
	<i>S. aureus</i> 503	CCARM 0205	2.5	5
	<i>S. aureus</i>	CCARM 3855	1.25	5
	<i>S. aureus</i>	CCARM 3089	5	5

Concentration unit: mg/mL.

### 3.6. Effect of THA-663S on Cell Viability and Cytoprotective

The cell viability effects of THA-663S (0.1, 1, and 10  $\mu$ g/mL) on UVB-irradiated cells were examined. As shown in Figure 3C, the protective was greater than 90% for all THA-663S concentrations, verifying that none of the tested concentrations of THA-663S were cytotoxic. Therefore, THA-663S concentrations ranging from 0.1–10  $\mu$ g/mL were used for further experiments.

Flow cytometry analysis demonstrated that intracellular ROS generation increased significantly in UVB-irradiated HaCaT cells, whereas this trend was decreased by THA-663S (Figure 3A,B). Compared with UVB-irradiated HaCaT cells, THA-663S was at 1, and 10  $\mu$ g/mL decreased ROS production by 20.6% and 21.4%, respectively.

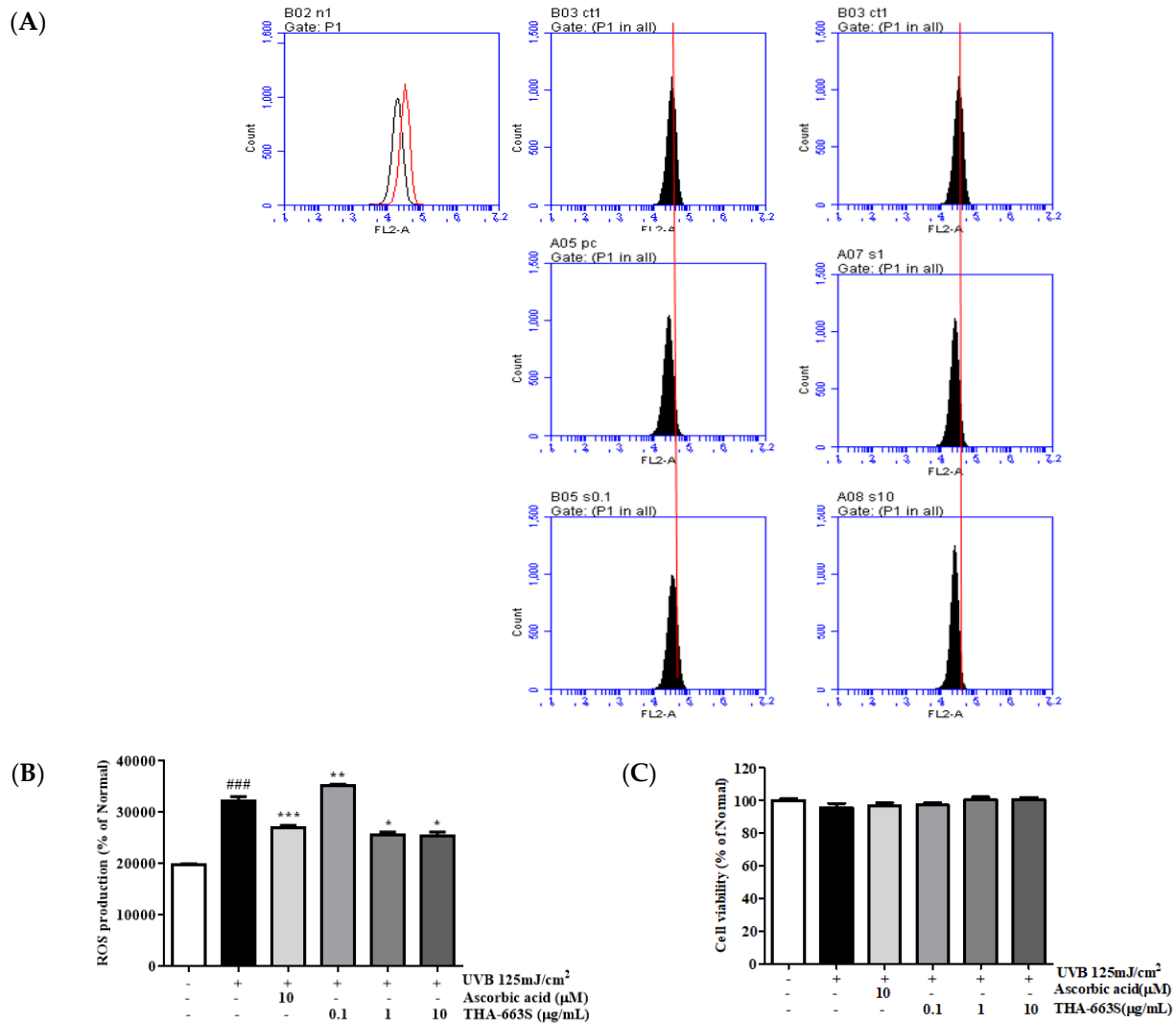


**Figure 3.** Cell viability and intracellular reactive oxygen species (ROS) generations in UVB-exposed HaCaT cells treated with THA-663S. Following UVB irradiation (125 mJ/cm<sup>2</sup>), HaCaT cells were THA-663. S (0.1, 1, and 10 µg/mL) for 24 h. ROS levels were determined using flow cytometry (A). The relative intensity of ROS generation is shown in the bar graph (B). Cell viability was measured using an MTT assay (C). The results were shown as the mean ± SD of three independent experiments. ###  $p < 0.001$  compared with non-irradiated group, \*  $p < 0.05$ , \*\*  $p < 0.01$ , \*\*\*  $p < 0.001$  compared with only UVB-irradiated group.

### 3.7. Effect of THA-663S on MMP-1 and MMP-3 Secretion in UVB-Irradiated HaCaT Cells

To assess the effects of THA-663S on UVB-irradiated MMP-1 and MMP-3 in HaCaT cells, the MMP-1 and MMP-3 secretions in the supernatant were measured using an ELISA kit. As indicated in Figure 4, the levels of MMP-1 and MMP-3 in the cells treated using UVB irradiation were higher than those of the normal group. However, at 10 µg/mL THA-663S MMP-1 and MMP-3 secretion reduced by 16.2% and 25.4%, respectively. Especially, THA-663S 10 µg/mL verified that the secretion amount of MMP-3 was further decreased by 7.5% compared with ascorbic acid, a positive control.

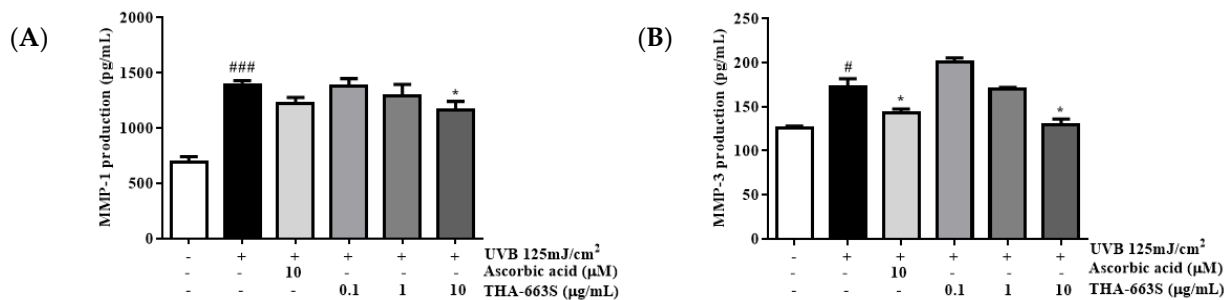


**Figure 4.** THA-663S inhibited the secretion of MMP-1 and MMP-3 in UVB-irradiated HaCaT cells. Following UVB irradiation (125 mJ/cm<sup>2</sup>), HaCaT cells were treated with or without the indicated concentration of THA-663S (0.1, 1, and 10 µg/mL) for 24 h. MMP-1 (A) and MMP-3 (B) levels were determined using ELISA kits. The results are shown as the mean ± SD of three independent experiments. #  $p < 0.05$ , ###  $p < 0.001$  compared with non-irradiated group, \*  $p < 0.05$  compared with only UVB-irradiated group.

### 3.8. Effect of THA-663S on MMP-1, TGF-β1, and Procollagen Type I mRNA Expression in UVB-Irradiated HaCaT Cells

To make the skin photoaging effects of THA-663S explicit, the mRNA levels of MMP-1, TGF-β1, and procollagen type I were further measured using RT-PCR. The mRNA level of MMP-1 in UVB-irradiated HaCaT cells was also markedly moved up, compared with that of non-irradiated cells, whereas 1-µg/mL THA-663S reduced UVB-induced MMP-1 by 64.7%, compared with the UVB-irradiated group (Figure 5). In contrast, UVB irradiation inhibited TGF-β1 mRNA expression, compared with the normal group. Interestingly, 1-µg/mL THA-663S increased UVB-irradiated TGF-β1 by 62.7%. However, in the case of procollagen type I, there was no tendency to grow. Based on the above results, THA-663S affects aging because of the photodamage caused by UVB. Therefore, further research on the biological mechanism of THA-663S was conducted.

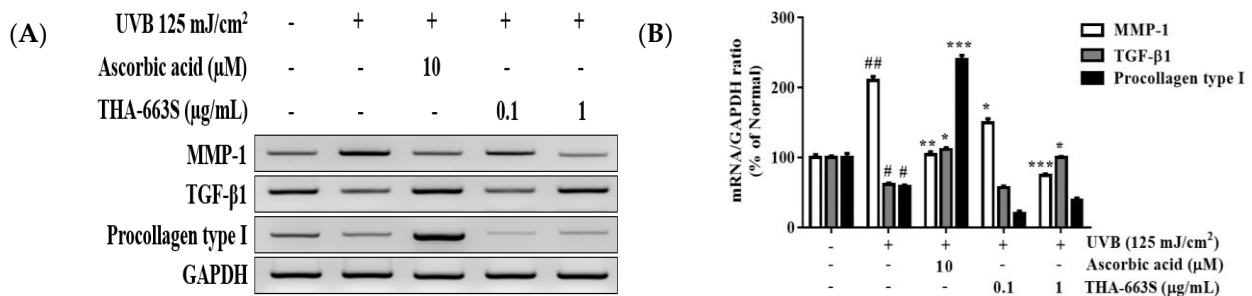


**Figure 5.** MMP-1, TGF-β1, and procollagen type I mRNA expression on HaCaT cells of THA-663S. Following UVB irradiation (125 mJ/cm<sup>2</sup>), HaCaT cells were treated with or without the shown concentrations of THA-663S (0.1 and 1 µg/mL) for 24 h. The MMP-1, TGF-β1, and procollagen type I mRNA levels were measured using RT-PCR analysis (A). The band intensities were quantified by densitometry, normalized to the level of GAPDH, and calculated as the percentage of the non-irradiated group (B). The results are shown as the mean ± SD of three independent experiments. #  $p < 0.05$ , ##  $p < 0.01$  compared with non-irradiated group, \*  $p < 0.05$ , \*\*  $p < 0.01$ , \*\*\*  $p < 0.001$  compared with only UVB-irradiated group.

### 3.9. Effect of THA-663S on Protein Expression of MAPK/AP-1 Signaling Pathway

When ROS triggers the activation of MAPK signaling plays an essential role in regulating MMP expression [22]. To investigate the molecular mechanisms by which THA-663S decreases MMP-1 and -3 levels, the phosphorylation of p38, ERK, and JNK was assessed. The results show that the UVB-induced phosphorylation of p38, ERK, and JNK was lower in THA-663S-treated cells compared with the UVB-irradiated control (Figure 6A,B). Especially, it was confirmed that the phosphorylation of p38, ERK, and JNK decreased by 57.5%, 96.6%,

and 74%, respectively, at 10  $\mu\text{g}/\text{mL}$  concentrations. These results suggest that THA-663S decreases MMP-1 expression by inhibiting the p38, ERK, and JNK pathways.

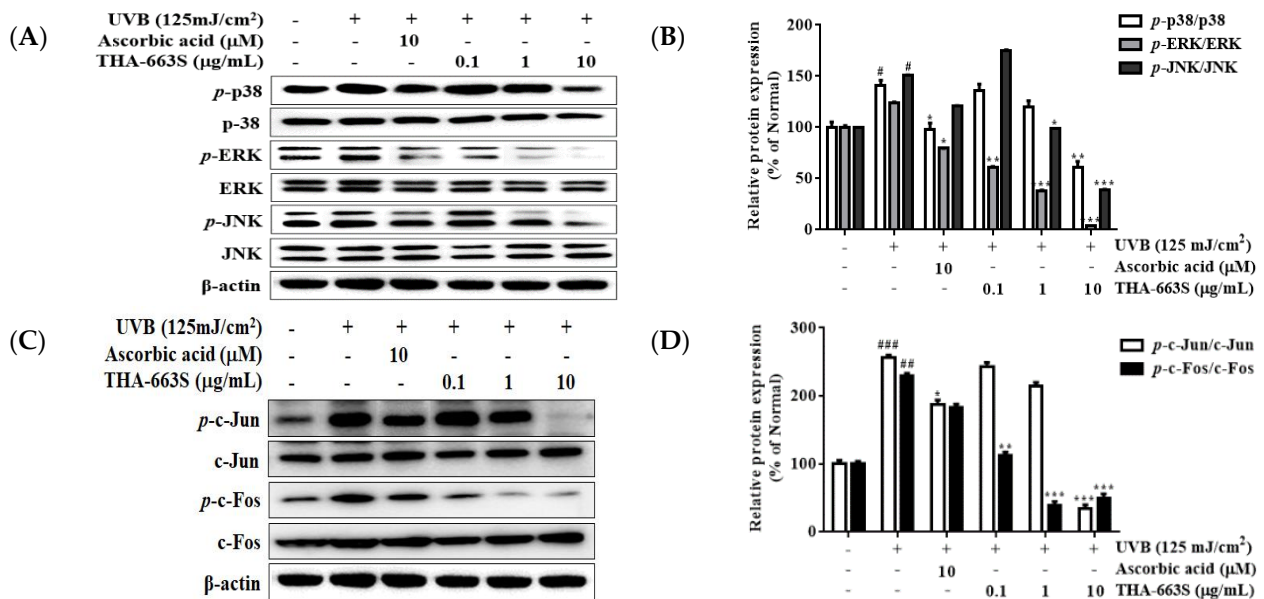


**Figure 6.** MAPK and AP-1 signaling protein expression in HaCaT cells of THA-663S. Following UVB irradiation (125 mJ/cm<sup>2</sup>), HaCaT cells were treated with or without the indicated concentration of THA-663S (0.1, 1, and 10  $\mu\text{g}/\text{mL}$ ) for 1.5 h and 4 h. The p-p38, p-ERK, and p-JNK protein levels were measured using Western blotting (A). The band intensities were quantified by densitometry, normalized to the level of  $\beta$ -actin, and calculated as the percentage of the non-irradiated group (B). The p-c-jun and p-c-fos protein levels were measured using Western blot (C). The band intensities were quantified by densitometry, normalized to the level of  $\beta$ -actin, and calculated as the percentage of the non-irradiated group (D). The results are shown as the mean  $\pm$  SD of three independent experiments. #  $p < 0.05$ , ##  $p < 0.01$ , ###  $p < 0.001$  compared with non-irradiated group, \*  $p < 0.05$ , \*\*  $p < 0.01$ , \*\*\*  $p < 0.001$  compared with only UVB-irradiated group.

The transcription factor AP-1 comprises the c-jun and c-fos proteins. MAPK activation leads to the expression and phosphorylation of c-jun and c-fos and transcriptional activation of MMP promoters. Therefore, levels of c-jun, c-fos, and phosphorylated c-jun and c-fos were determined after UVB irradiation and THA-663S treatment using Western blotting. Treatment with THA-663S at 10  $\mu\text{g}/\text{mL}$  supplied the most inhibition on phosphorylated AP-1. Particularly, treatment with THA-663S decreased p-c-jun and p-c-fos expression by 86.8% and 78.3%, respectively (Figure 6C,D).

### 3.10. Effect of THA-663S on Protein Expression of TGF- $\beta$ /Smad Signaling Pathway

Smad proteins and TGF- $\beta$  play a crucial role in the TGF- $\beta$ -dependent regulation of collagen and the control of other ECM components [23]. Especially, Smad 7 (as a negative feedback inhibitor) can work against Smad 2 and Smad 3 for binding to activated TGF $\beta$ 1 and, thus, decrease TGF- $\beta$ /Smad signaling. The regulation of TGF- $\beta$ /Smad7 signaling pathway proteins by THA-663S was measured using Western blotting. The protein level of TGF- $\beta$ 1 was increased by 303.4% at 10  $\mu\text{g}/\text{mL}$ , whereas Smad7 level was decreased by 91.6% at 10  $\mu\text{g}/\text{mL}$  in THA-663S-treated cells compared with the UV-irradiated control, suggesting that THA-663S downregulates Smad7 expression and upregulates TGF- $\beta$ 1 expression (Figure 7).

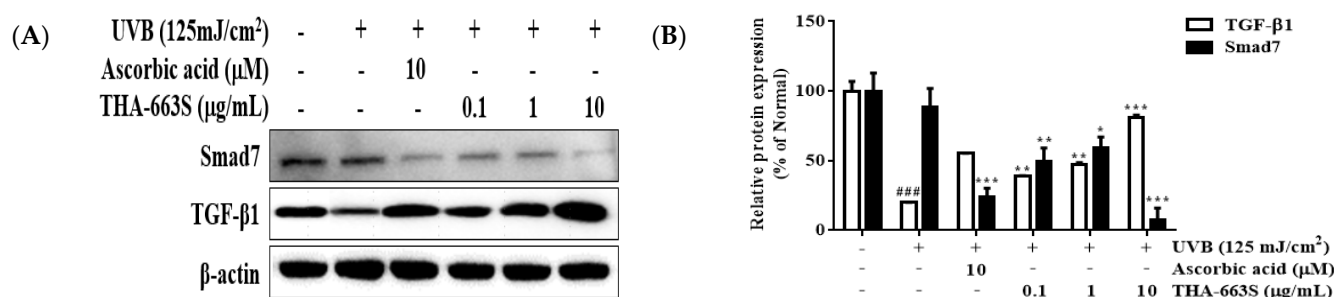


**Figure 7.** TGF- $\beta$ /Smad signaling protein expression in HaCaT cells of THA-663S. Following UVB irradiation (125 mJ/cm<sup>2</sup>), HaCaT cells were treated with or without the indicated concentration of THA-663S (0.1, 1, and 10  $\mu$ g/mL) for 1.5 h. The TGF- $\beta$ 1 and Smad7 protein levels were measured using Western blotting (A). The band intensities were quantified using densitometry, normalized to the level of  $\beta$ -actin, and calculated as the percentage of the non-irradiated group (B). The results are shown as the mean  $\pm$  SD of three independent experiments. ###  $p < 0.001$  compared with non-irradiated group, \*  $p < 0.05$ , \*\*  $p < 0.01$ , \*\*\*  $p < 0.001$  compared with only UVB-irradiated group.

#### 4. Discussion

*Streptomyces* is a valuable industrial microorganism group recognized for its application and importance in developing modern drugs [24]. This study focused on anti-aging and antibacterial activities, and the primary purpose was to select bacteria with effective protection and treatment potential for human skin.

The 16S rRNA sequencing results showed that the strain *S. chattanoogensis* THA-663 was closely related to *Streptomyces lydicus* ATCC 25470 (99.85% sequence similarity), *Streptomyces chattanoogensis* NRRL ISP-5002 (99.85%), and *Streptomyces sioyaensis* NRRL B-5408 (99.34%), and its extract can inhibit MRSA strains with great antibacterial effect at the concentration of 10 mg/mL (Figure 1).

Most scientific reports suggest the role of compounds such as antioxidants, vitamins, and enzymes in keeping the skin rejuvenating for a longer period. Therefore, treating the skin with antioxidant ingredients obtained from microbes may be a useful strategy for preventing UVB-irradiated cutaneous damage. Our results show that the inhibitory activity of DPPH- and ABTS-free scavenging radicals was detectable at IC<sub>50</sub> values of 521.2 and 160.5 ppm, respectively (Figure 2). After treatment using THA-663S, the level of ROS was significantly dose-dependently reduced (Figure 3A,B). The ability of THA-663S to scavenge DPPH and ABTS radicals was superior to that of ascorbic acid. This well-known skin brightener was used as a positive control.

In addition, UV radiation-induced ROS trigger an increase in MMPs, degrade ECM proteins, such as collagen and elastin, and lead to skin photoaging and wrinkle formation [25]. To assess the effect of pre-and post-enzyme-treated THA-663S on UVB-induced photoaging, the mRNA expression of MMP-1 and procollagen type I in UVB-irradiated HaCaT cells was investigated using RT-PCR. Our results showed that THA-663S recovered the expression of procollagen type I (Figure 5) and significantly reduced MMP-1 expression in UVB-irradiated HaCaT cells. These findings suggest that THA-663S prevents collagen loss by inhibiting UVB-induced MMP-1 expression and enhancing procollagen type I expression.

Keratinocytes, the predominant cell type in the epidermis, absorb most UVB irradiation, leading to dryness, loosening, and inflammation [26]. The UVB irradiation of the epidermis causes ROS generation, which increases MMP-1 and MMP-3 secretion. In this study, THA-663S treatment in HaCaT cells undergoing UVB irradiation resulted in decreases in MMP-1 and MMP-3 secretion. Compared with UVB-irradiated HaCaT cells, at 10  $\mu$ g/mL THA-663S, MMP-1 and MMP-3 secretion reduced by 16.2% and 25.4%, respectively (Figure 4). These results of THA-663S indicate a similar pattern with the experimental results of *Sambucus nigra* L. extract by Pei Lin et al. [27]. Therefore, we can confirm that THA-663 has potential anti-aging qualities.

The MAPK signaling pathway plays a crucial role in regulating MMP expression, cell proliferation, differentiation, and death [28]. AP-1, as a MAPK downstream activator, is a well-known transcription factor that stimulates the gene transcription of MMPs [29]. THA-663S indicated that the deglycosylated products showed stronger activity than their respective counterparts in inhibiting UVB radiation-induced phosphorylation of ERK, JNK, p-38, and p-c-fos, and p-c-jun expression in HaCaT cells (Figure 6). Lu Li et al. [30] and Choi HJ et al. [31] reported UVB-induced MAPK/AP-1 expression in HaCaT cells. Similarly, our results showed that THA-663S regulated the MAPK and AP-1 signaling pathways. Components of the TGF- $\beta$  pathway itself are reduced in aged human skin. Alternatively, Smad7 proteins have a significant negative regulation of the TGF- $\beta$ /SMAD pathway. Specifically, the levels of TGF- $\beta$ 1 reduced by 79.9% following UVB irradiation, which was recovered with 10  $\mu$ g/mL THA-663S treatment by 303.4%. Smad7 expression was reduced by 11.5% following UVB irradiation, and this decrease was reduced to 91.6% in the presence of 10  $\mu$ g/mL THA-663S (Figure 7) These results also support that THA-663 is an effective substance in protecting skin barrier and anti-aging.

Antibacterial preservatives are added to cosmetics to maintain a microbe-free status throughout the use period, and natural antibacterial compounds with various functions are better and more beneficial for human health. Particularly, secondary metabolites obtained from bacteria are more easily accessible because of their ease of production and production cost. As this study aimed to evaluate the cosmetic potential of antioxidants, anti-aging, and bacterial strains THA-663S, the main goal was to develop final cosmetics or treatments for local applications using bioactive materials extracted from soil microorganisms.

MRSA spread mainly in hospitals in the early days, but now MRSA is found even in unrelated places, emerging as a big problem. Death from MRSA is on the rise every year, and new antibiotics are being urgently developed. MRSA is a frequently identified strain in infected wounds and is an important skin elasticity factor. Woo YK et al. [32] suggested that if there is an antibacterial activity against MRSA, the possibility of application as an antibacterial cosmetic material is excellent. It was verified that THA-663S showed excellent antibacterial activity against MRSA and had significant anti-aging effects on the skin with no cytotoxicity (Tables 3 and 5 and Figure 3C). Therefore, its positive effects on infection prevention and treatment could be shown when applied to skin diseases and wounds specifically caused by MRSA.

Identification of secondary metabolites was performed on the basis of the analysis of THA-663S using UPLC-QTOF/MS. As a result of conducting a component analysis of THA-663S with UPLC-Qtof-MS, seven confirmed compounds are listed in Table 4. Compounds CHEMBL184245 [33] and CHEMBL83512 [34] are reported to have antibacterial activity for MRSA, CHEMBL2148184 has an anti-inflammatory effect [35], and CHEMBL2299266 [36] has antioxidant activity.

In conclusion, this paper provides many lines of scientific evidence regarding the anti-photoaging effects of THA-663S on UVB-exposed skin. Our results showed that THA-663S metabolite extraction modulates many signaling pathways related to skin photoaging by downregulating collagen degradation and stimulating collagen synthesis. Therefore, THA-663S is expected to be applicable to functional foods, cosmetic products, and medicines as a dual-functional material for improving human skin disorders, due to its anti-bacterial and anti-photoaging effects.

## 5. Conclusions

This study aimed to identify *Streptomyces* species isolated from the soil and to study the anti-aging effects and mechanism in vitro. The result of the taxonomic study identified that the isolated strain THA-663 was *S. chattanoogensis*. THA-663S was confirmed as including methyl palmitate, mevalonolactone, oleamide, and sulfurol by GC-MS, and CHEMBL184245, CHEMBL2148184, CHEMBL83512, kenganthranol A, CHEMBL1484171, and CHEMBL2299266 were detected by UPLC-Qtof-MS.

The results showed that THA-663S blocked the upregulated production of the ROS induced in UVB-irradiated HaCaT cells. Treatment with THA-663S also significantly ameliorated the mRNA expression of MMPs and procollagen type I. The phosphorylation level of c-jun and c-fos was also decreased through the attenuated expression of p-38, p-ERK, and p-JNK after treatment with THA-663S. In addition, the treatment of THA-663S resulted in the inhibition of Smad7 expression in the TGF- $\beta$ /Smad pathway. Hence, the synthesis of procollagen type I, a precursor of collagen I, was promoted. Those results meant that the isolated strain *S. chattanoogensis* THA-663's metabolite had great anti-aging activity on the skin. In addition, THA-663S showed an anti-bacterial effect on Gram-positive coccus bacteria, *S. aureus*. Moreover, it showed anti-bacterial activity on MRSA, which is expected to play an important role in skin infection and recovery after infection. In conclusion, the isolated strain *S. chattanoogensis* THA-663's metabolites extraction showed a great possibility as an anti-aging and skin-related drug candidate.

**Supplementary Materials:** The following supporting information can be downloaded at: <https://www.mdpi.com/article/10.3390/cosmetics9060126/s1>. Table S1: List of methicillin-resistant *Staphylococcus aureus*; Table S2: Oligonucleotide primers used for RT-PCR.

**Author Contributions:** Conceptualization, T.-H.Y., S.Z. and S.O.; methodology, S.Z. and M.F.; software, S.O., S.Z. and T.T.M.N.; validation, S.O., M.F. and S.Z.; formal analysis, S.Z., S.O. and M.F.; investigation, T.-H.Y., S.O. and J.J. (Jeehaeng Jeong); resources, A.D.B., J.J. (Jeyong Jung) and T.T.M.N.; data curation, S.Z., J.J. (Jeyong Jung) and M.F.; writing—S.O. and A.D.B.; writing—review and editing, T.-H.Y. and S.O.; visualization, S.Z., A.D.B., T.T.M.N. and J.J. (Jeyong Jung); supervision, T.-H.Y. and J.J. (Jeehaeng Jeong); project administration, T.-H.Y. and J.J. (Jeehaeng Jeong). All authors have read and agreed to the published version of the manuscript.

**Funding:** This research received no external funding.

**Institutional Review Board Statement:** Not applicable.

**Informed Consent Statement:** Not applicable.

**Data Availability Statement:** The data presented in this study are available in this paper.

**Acknowledgments:** This research was kindly supported by Snow White Factory.

**Conflicts of Interest:** The authors declare no conflict of interest.

## References

1. Ganceviciene, R.; Liakou, A.I.; Theodoridis, A.; Makrantonaki, E.; Zouboulis, C.C. Skin anti-aging strategies. *Derm.-Endocrinol.* **2012**, *4*, 308–319. [[CrossRef](#)]
2. Chambers, E.S.; Vukmanovic-Stejic, M. Skin barrier immunity and ageing. *Immunology* **2020**, *160*, 116–125. [[CrossRef](#)] [[PubMed](#)]
3. de Jager, T.L.; Cockrell, A.E.; Du Plessis, S.S. Ultraviolet Light Induced Generation of Reactive Oxygen Species. *Adv. Exp. Med. Biol.* **2017**, *996*, 15–23. [[PubMed](#)]
4. Kwon, K.-R.; Alam, M.B.; Park, J.-H.; Kim, T.-H.; Lee, S.-H. Attenuation of UVB-Induced Photo-Aging by Polyphenolic-Rich *Spatholobus Suberectus* Stem Extract via Modulation of MAPK/AP-1/MMPs Signaling in Human Keratinocytes. *Nutrients* **2019**, *11*, 1341. [[CrossRef](#)] [[PubMed](#)]
5. Tanaka, Y.; Uchi, H.; Furue, M. Antioxidant cinnamaldehyde attenuates UVB-induced photoaging. *J. Dermatol. Sci.* **2019**, *96*, 151–158. [[CrossRef](#)] [[PubMed](#)]
6. Jin, Y.-J.; Ji, Y.; Jang, Y.-P.; Choung, S.-Y. *Acer tataricum* subsp. *ginnala* Inhibits Skin Photoaging via Regulating MAPK/AP-1, NF- $\kappa$ B, and TGF $\beta$ /Smad Signaling in UVB-Irradiated Human Dermal Fibroblasts. *Molecules* **2021**, *26*, 662. [[CrossRef](#)]
7. Munshi, A.; Ramesh, R. Mitogen-Activated Protein Kinases and Their Role in Radiation Response. *Genes Cancer* **2013**, *4*, 401–408. [[CrossRef](#)] [[PubMed](#)]
8. Karin, M. The Regulation of AP-1 Activity by Mitogen-activated Protein Kinases. *J. Biol. Chem.* **1995**, *270*, 16483–16486. [[CrossRef](#)] [[PubMed](#)]
9. Cooper, S.J.; Bowden, G.T. Ultraviolet B regulation of transcription factor families: Roles of nuclear factor-kappa B (NF- $\kappa$ B) and activator protein-1 (AP-1) in UVB-induced skin carcinogenesis. *Curr. Cancer Drug Targets* **2007**, *7*, 325–334. [[CrossRef](#)]
10. Li, N.; Karin, M. Ionizing radiation and short wavelength UV activate NF- $\kappa$ B through two distinct mechanisms. *Proc. Natl. Acad. Sci. USA* **1998**, *95*, 13012–13017. [[CrossRef](#)]
11. He, T.; Quan, T.; Shao, Y.; Voorhees, J.J.; Fisher, G.J. Oxidative exposure impairs TGF- $\beta$  pathway via reduction of type II receptor and SMAD3 in human skin fibroblasts. *Age* **2014**, *36*, 9623. [[CrossRef](#)] [[PubMed](#)]

12. Quan, T.; He, T.; Voorhees, J.J.; Fisher, G.J. Ultraviolet Irradiation Blocks Cellular Responses to Transforming Growth Factor- $\beta$  by Down-regulating Its Type-II Receptor and Inducing Smad7. *J. Biol. Chem.* **2001**, *276*, 26349–26356. [[CrossRef](#)] [[PubMed](#)]
13. Omura, S.; Ikeda, H.; Ishikawa, J.; Hanamoto, A.; Takahashi, C.; Shinose, M.; Takahashi, Y.; Horikawa, H.; Nakazawa, H.; Osonoe, T.; et al. Genome sequence of an industrial microorganism *Streptomyces avermitilis*: Deducing the ability of producing secondary metabolites. *Proc. Natl. Acad. Sci. USA* **2001**, *98*, 12215–12220. [[CrossRef](#)] [[PubMed](#)]
14. Běhal, V. Bioactive products from *Streptomyces*. *Adv. Appl. Microbiol.* **2000**, *47*, 113–156.
15. Laube, S.; Farrell, A.M. Bacterial Skin Infections in the Elderly. *Drugs Aging* **2002**, *19*, 331–342. [[CrossRef](#)] [[PubMed](#)]
16. Fang, M.; Lee, H.M.; Oh, S.; Zheng, S.; Bellere, A.D.; Kim, M.; Choi, J.; Kim, M.; Yu, D.; Yi, T.H. *Rosa davurica* inhibits skin photoaging via regulating MAPK/AP-1, NF- $\kappa$ B, and Nrf2/HO-1 signaling in UVB-irradiated HaCaTs. *Photochem. Photobiol. Sci.* **2022**; Advance online publication. [[CrossRef](#)]
17. Flårdh, K.; Buttner, M.J. *Streptomyces* morphogenetics: Dissecting differentiation in a filamentous bacterium. *Nat. Rev. Microbiol.* **2009**, *7*, 36–49. [[CrossRef](#)] [[PubMed](#)]
18. Davoodbasha, M.; Edachery, B.; Nooruddin, T.; Lee, S.-Y.; Kim, J.-W. An evidence of C16 fatty acid methyl esters extracted from microalga for effective antimicrobial and antioxidant property. *Microb. Pathog.* **2018**, *115*, 233–238. [[CrossRef](#)]
19. Balouiri, M.; Sadiki, M.; Ibsouda, S.K. Methods for in vitro evaluating antimicrobial activity: A review. *J. Pharm. Anal.* **2016**, *6*, 71–79. [[CrossRef](#)]
20. Arifiyanto, A.; Surtiningsih, T.; Ni'Matuzahroh; Fatimah; Agustina, D.; Alami, N.H. Antimicrobial activity of biosurfactants produced by actinomycetes isolated from rhizosphere of Sidoarjo mud region. *Biocatal. Agric. Biotechnol.* **2020**, *24*, 101513. [[CrossRef](#)]
21. Sahin, N. Antimicrobial activity of *Streptomyces* species against mushroom blotch disease pathogen. *J. Basic Microbiol.* **2005**, *45*, 64–71. [[CrossRef](#)]
22. Wang, Z.; Li, Y.; Sarkar, F.H. Signaling mechanism(s) of reactive oxygen species in Epithelial-Mesenchymal Transition reminiscent of cancer stem cells in tumor progression. *Curr. Stem Cell Res. Ther.* **2010**, *5*, 74–80. [[CrossRef](#)] [[PubMed](#)]
23. Verrecchia, F.; Mauviel, A. Transforming growth factor-beta signaling through the Smad pathway: Role in extracellular matrix gene expression and regulation. *J. Investig. Dermatol.* **2002**, *118*, 211–215. [[CrossRef](#)] [[PubMed](#)]
24. Chater, K.F. *Streptomyces* inside-out: A new perspective on the bacteria that provide us with antibiotics. *Philos. Trans. R. Soc. B Biol. Sci.* **2006**, *361*, 761–768. [[CrossRef](#)]
25. Gromkowska-Kępcza, K.J.; Puścion-Jakubik, A.; Markiewicz-Żukowska, R.; Socha, K. The impact of ultraviolet radiation on skin photoaging—Review of in vitro studies. *J. Cosmet. Dermatol.* **2021**, *20*, 3427–3431. [[CrossRef](#)] [[PubMed](#)]
26. Brandner, J.; Zorn-Kruppa, M.; Yoshida, T.; Moll, I.; Beck, L.; De Benedetto, A. Epidermal tight junctions in health and disease. *Tissue Barriers* **2014**, *3*, e974451. [[CrossRef](#)]
27. Lin, P.; Hwang, E.; Ngo, H.T.T.; Seo, S.A.; Yi, T.H. *Sambucus nigra* L. ameliorates UVB-induced photoaging and inflammatory response in human skin keratinocytes. *Cytotechnology* **2019**, *71*, 1003–1017. [[CrossRef](#)]
28. Yang, M.; Huang, C.Z. Mitogen-activated protein kinase signaling pathway and invasion and metastasis of gastric cancer. *World J. Gastroenterol.* **2015**, *21*, 11673–11679. [[CrossRef](#)]
29. Cargnello, M.; Roux, P.P. Activation and Function of the MAPKs and Their Substrates, the MAPK-Activated Protein Kinases. *Microbiol. Mol. Biol. Rev.* **2011**, *75*, 50–83. [[CrossRef](#)]
30. Li, L.; Hwang, E.; Ngo, H.T.T.; Lin, P.; Gao, W.; Liu, Y.; Yi, T.-H. Antiphotaging Effect of *Prunus yonesis* Blossom Extract via Inhibition of MAPK/AP-1 and Regulation of the TGF- $\beta$ 1/Smad and Nrf2/ARE Signaling Pathways. *Photochem. Photobiol.* **2018**, *94*, 725–732. [[CrossRef](#)]
31. Choi, H.-J.; Alam, M.B.; Baek, M.-E.; Kwon, Y.-G.; Lim, J.-Y.; Lee, S.-H. Protection against UVB-Induced Photoaging by *Nyssa fruticans* via Inhibition of MAPK/AP-1/MMP-1 Signaling. *Oxid. Med. Cell. Longev.* **2020**, *2020*, 2905362. [[CrossRef](#)]
32. Woo, Y.K.; Park, J.; Ryu, J.H.; Cho, H.J. The anti-inflammatory and anti-apoptotic effects of advanced anti-inflammation composition (AAIC) in heat shock-induced human HaCaT keratinocytes. *J. Cosmet. Dermatol.* **2020**, *19*, 2114–2124. [[CrossRef](#)] [[PubMed](#)]
33. Shin, D.Y.; Kim, S.N.; Chae, J.H.; Hyun, S.S.; Seo, S.Y.; Lee, Y.S.; Lee, K.O.; Kim, S.H.; Lee, Y.S.; Jeong, J.M.; et al. Syntheses and anti-MRSA activities of the C3 analogs of mansonone F, a potent anti-bacterial sesquiterpenoid: Insights into its structural requirements for anti-MRSA activity. *Bioorg. Med. Chem. Lett.* **2004**, *14*, 4519–4523. [[CrossRef](#)] [[PubMed](#)]
34. Fortuna, C.G.; Bonaccorso, C.; Bulbarelli, A.; Caltabiano, G.; Rizzi, L.; Goracci, L.; Musumarra, G.; Pace, A.; Piccionello, A.P.; Guarcello, A.; et al. New linezolid-like 1,2,4-oxadiazoles active against Gram-positive multiresistant pathogens. *Eur. J. Med. Chem.* **2013**, *65*, 533–545. [[CrossRef](#)] [[PubMed](#)]
35. Zhang, S.; Cheng, K.; Wang, X.; Yin, H. Selection, synthesis, and anti-inflammatory evaluation of the arylidene malonate derivatives as TLR4 signaling inhibitors. *Bioorg. Med. Chem.* **2012**, *20*, 6073–6079. [[CrossRef](#)] [[PubMed](#)]
36. Gutierrez, R.M.P. Antihepatotoxic, nephroprotective, and antioxidant activities of phenolic compounds from *Satureja macrostema* leaves against carbon tetrachloride-induced hepatic damage in mice. *Med. Chem. Res.* **2013**, *22*, 1846–1855. [[CrossRef](#)]